frontiers in Plant Science

TYPE Original Research
PUBLISHED 09 March 2026
DOI 10.3389/fpls.2026.1767323

Check for updates

OPEN ACCESS

EDITED BY
Vladimir Orbovic,
University of Florida, United States

REVIEWED BY
Aleš Soukup,
Charles University, Czechia
Shannon Barry,
University of Florida, United States

*CORRESPONDENCE
Wenjin Yu
yuwjin@gxu.edu.cn

RECEIVED 14 December 2025
REVISED 21 February 2026
ACCEPTED 23 February 2026
PUBLISHED 09 March 2026

CITATION
Lan W, Chen H, Zou B, Yi Q, Lin X, Xu J, Lei T, Zhang J, Chen X, Wang P and Yu W (2026) A non-destructive plant screening method for improving sample uniformity in horticultural crops based on a hydrogen peroxide fluorescent probe. *Front. Plant Sci.* 17:1767323. doi: 10.3389/fpls.2026.1767323

COPYRIGHT
© 2026 Lan, Chen, Zou, Yi, Lin, Xu, Lei, Zhang, Chen, Wang and Yu. This is an open-access article distributed under the terms of the Creative Commons Attribution License (CC BY). The use, distribution or reproduction in other forums is permitted, provided the original author(s) and the copyright owner(s) are credited and that the original publication in this journal is cited, in accordance with accepted academic practice. No use, distribution or reproduction is permitted which does not comply with these terms.

A non-destructive plant screening method for improving sample uniformity in horticultural crops based on a hydrogen peroxide fluorescent probe

Weisen Lan[1], Hongjie Chen[2], Bingying Zou[1], Qingyuan Yi[3], Xia Lin[4], Junrong Xu[1], Tianying Lei[1], Junwei Zhang[1], Xinyuan Chen[1], Peng Wang[1] and Wenjin Yu[1]*

[1]College of Agriculture, Guangxi University, Nanning, China, [2]School of Energy and Building Environment, Guilin University of Aerospace Technology, Guilin, China, [3]Medical College, Guangxi University, Nanning, China, [4]Faculty of Pharmacy, Guangxi Health Science College, Nanning, China

Introduction: Hydrogen peroxide (H_2O_2) functions as a key signaling molecule in plants responding to stress. Although numerous detection methods have been developed, simple and non-destructive techniques for the semi-quantitative monitoring of H_2O_2 in plant tissues remain scarce.

Methods: In this study, we developed a "turn-on" fluorescent probe specifically designed to detect endogenous H_2O_2 in plant tissues, and conducted spectroscopic and in vivo toxicity tests. Furthermore, under experimentally controlled stress conditions, we utilized this probe to detect H_2O_2 levels in four distinct plant types exposed to salt, waterlogging, cadmium, and drought stresses. Additionally, H_2O_2 was detected in a grafting model under non-experimentally controlled stress conditions.

Results: The results showed that the probe demonstrated excellent selectivity, a strong linear correlation (R2 = 0.9849), and a low detection limit of 0.6450 μmol/L. Importantly, it exhibits good biocompatibility with plant tissues and effectively minimizes detection errors caused by transient H_2O_2 fluctuations induced by environmental changes. Consequently, it provides more accurate and stress-reflective H_2O_2 measurements. Under experimentally controlled stress conditions, the changes in relative fluorescence intensity conformed to the typical response patterns observed when plants experience graded levels of stress. Notably, even under complex grafting conditions without imposed stress gradients, applying the probe to bottle gourd (Lagenaria siceraria) rootstocks with different graft compatibility produced fluorescence dynamics consistent with the typical H_2O_2 responses of compatible and incompatible rootstocks, and the distribution of relative fluorescence intensity within the population underscored the importance of prescreening plants for biological studies. Pearson correlation and Bland-Altman analyses confirmed good agreement between our method and the commercial assay kit.

Discussion: These results demonstrate that the LWS probe enables H_2O_2 detection and, in combination with the IVIS in vivo imaging system, can screen individual plants differing in stress responses more effectively than other sensors.

This non-destructive approach preserves the structural integrity of plant samples, enabling follow-up physiological, biochemical, and genomic analyses on the same specimens. This method provides a reliable prescreening platform for investigating plant stress responses at the biological level.

KEYWORDS
fluorescent probe, H_2O_2, nondestructive, plants, prescreening, semi-quantitative

1 Introduction

With the intensification of global climate change and environmental pressures, plants are increasingly subjected to both biotic and abiotic stresses, such as drought, salinity, elevated temperatures, and pathogen infections. These stresses pose significant threats to plant growth, development, and yield. Therefore, gaining an in-depth understanding of the mechanisms underlying plant stress resistance is crucial for improving crop adaptability (Cotrina Cabello et al., 2023; Ahlawat et al., 2024). In recent years, omics technologies have provided powerful tools for studying plant stress resistance mechanisms. However, current omics sampling strategies primarily rely on fixed time points following stress treatment, overlooking the variability among individual plants (Shulaev et al., 2008; Muthamilarasan et al., 2019). Inter-individual variability in plants is a critical issue in biological research. Even within the same cultivar, under identical environmental conditions and uniform stress treatments, significant differences can arise in both response timing and intensity. Specifically, some individuals may not yet reach their maximum response at predefined sampling points, while others may have already passed their peak response. This temporal asynchrony introduces samples that are inconsistent with the targeted oxidative status, ultimately affecting the accuracy and reliability of omics data. (Cortijo et al., 2019; Schupp et al., 2019; Watahiki and Trewavas, 2019) Therefore, improving the uniformity of physiological states contributes to enhancing data quality and analytical accuracy. Furthermore, current research on plant stress resistance mechanisms typically involves the propagation of multiple plant generations, enabling the selection of individuals or varieties with varying resistance levels for further analysis. These plants exhibit differences in substances such as H_2O_2, plant hormones, antioxidants, and other related compounds (Asaeda et al., 2017; Liaqat et al., 2024). Conventional screening methods for disease-resistant plant varieties predominantly rely on the observation of typical symptom development induced by pathogens under field conditions. However, the monitoring and evaluation of disease symptoms throughout the entire growing season can require a long period of time, and visual assessments may not consistently and accurately reflect the resistance levels, as certain resistant plants may still exhibit mild symptoms at the sampling time points (Tibebu and Nuh, 2019; Jennings et al., 2024). Following stress exposure, physiological changes in plants occur earlier than the onset of visible symptoms. Quantitative measurements of these physiological parameters provide objective data, ensuring more reliable results compared to evaluations that depend on visible symptoms (Mutka and Bart, 2015). Consequently, physiological profiling of plant stress responses enables precise identification of resistant phenotypes, significantly accelerating the selection process in breeding programs aimed at developing stress-resilient crop varieties.

Elevation of reactive oxygen species (ROS) levels represents one of the most prominent physiological alterations in plants exposed to various biotic and abiotic stresses in natural environments. ROS encompass a group of redox-active molecules, primarily comprising H_2O_2, superoxide anion ($\cdot O_2^-$), hydroxyl radical (·OH), and nitric oxide radical (NO·) (Hasanuzzaman et al., 2021). Under normal physiological conditions, ROS in plant cells are maintained at low levels through the regulatory action of the antioxidant system. Upon exposure to stress, ROS production rates are dramatically enhanced, exceeding the scavenging capacity of the antioxidant system and consequently leading to a marked elevation in ROS accumulation. Such ROS accumulation activates a series of signal transduction pathways, triggering plant defense responses and adaptive mechanisms (Farooq et al., 2019). H_2O_2 represents the most stable ROS, characterized by an extended half-life and superior diffusion capacity (Sharova et al., 2023; Henschel et al., 2024). This enables H_2O_2 to function not only as a local signaling molecule within cells but also to be transported over long distances through the apoplast and intercellular spaces, mediating intercellular signal transmission. As a result, plants are able to coordinate responses across different tissues and organs, thereby enhancing overall stress resistance (Slesak et al., 2007). As a signaling molecule, H_2O_2 can regulate the secretion of plant hormones in a dose-dependent manner, thereby influencing plant growth, development, and defense responses. Low concentrations of H_2O_2 typically promote plant growth and development, moderate concentrations can induce defense responses, while high concentrations may cause cellular damage or even cell death (Saxena et al., 2016; Nazir et al., 2020). Therefore, H_2O_2 serves as an indicator of the extent of plant damage and acts as a key determinant in the regulation of other plant hormones. Non-destructive assessment of H_2O_2 concentrations in plants can facilitate a better understanding of plant responses to stress and assist in the selection of more stress-tolerant individuals, thereby significantly enhancing breeding efficiency.

Traditional methods for detecting H_2O_2, such as chemiluminescence, electrochemical techniques, and chromatography, offer high sensitivity and accuracy but typically require destructive sampling of plant tissues. This limitation prevents the use of the same batch of samples for further studies, even when the response trends of plants under stress have been identified. Fluorescent proteins, as a non-invasive approach for detecting H_2O_2, can be expressed in living cells to emit fluorescence.

However, their low transformation efficiency and unstable expression levels have restricted their widespread application in practical settings (Li et al., 2021; Mizuta, 2021). Small-molecule fluorescent probes have become currently among the most widely used non-invasive methods for detecting H_2O_2. These probes generate a fluorescent signal upon reaction with H_2O_2, enabling the monitoring of H_2O_2 concentration changes without causing destructive damage to the target being observed (Yang et al., 2023). Fluorescent probes for H_2O_2 detection commonly utilize boronate esters and their derivatives as recognition groups. Upon attack of the boron atom by H_2O_2, the boron-carbon bond is cleaved, releasing the corresponding phenolic derivative and altering the properties of the fluorescent probe, thereby enabling H_2O_2 detection. However, boronate esters are prone to hydrolysis in aqueous solutions, which can affect the synthesis and storage of the probes. Consequently, the preparation of fluorescent probes containing boronate groups requires researchers to possess extensive expertise and proficient synthetic skills, making such probes less accessible for agricultural and forestry scientists (Dhoun et al., 2017; Liang et al., 2021; Kirchner et al., 2024; Peng et al., 2024). Other fluorescent probes that employ acetyl, sulfonate, benzoyl, and similar groups as recognition moieties avoid the hydrolysis issues associated with boronate esters during synthesis and can be used to monitor oxidative stress changes in living organisms. However, these probes are predominantly utilized for the qualitative analysis of H_2O_2, making precise comparisons and statistical analyses difficult. This limitation restricts in-depth studies on the role of H_2O_2 and the biological responses it triggers (Wu et al., 2019; Yin et al., 2022; Li et al., 2023a, b; Wang et al., 2023). Although these probes have demonstrated excellent performance and some H_2O_2 fluorescent probes have been applied to plants, especially in imaging on plant root tips, the results are encouraging. However, these works lack simple and easily reproducible procedures and methods for the semi-quantitative detection of H_2O_2 in biological organisms while preserving intact plants. As a result, researchers in the fields of agriculture and forestry have shown little interest in these works, which has limited the application of fluorescent probe technology in the agricultural and forestry sectors.

In this study, a novel fluorescent probe for detecting H_2O_2 in plants was synthesized using a rhodamine derivative and pentafluorobenzenesulfonyl chloride as raw materials through a two-step chemical reaction (Figure 1a). Using this probe in combination with the IVIS Lumina LT *in vivo* imaging system, H_2O_2 levels in different parts of intact plants can be detected with only simple sample preparation, while preserving the integrity of the plant. Quantitative results reflecting relative fluorescence intensity changes induced by H_2O_2 can be obtained (Figures 1b, c). This new probe, together with the IVIS Lumina LT system, demonstrates promising potential for assisting researchers in the agricultural and forestry fields in screening plants exhibiting different degrees of damage.

2 Materials and methods

2.1 Experimental instruments and reagents

All analytical instruments were used as specified: nuclear magnetic resonance (NMR) spectrometer (AVANCE NEO,

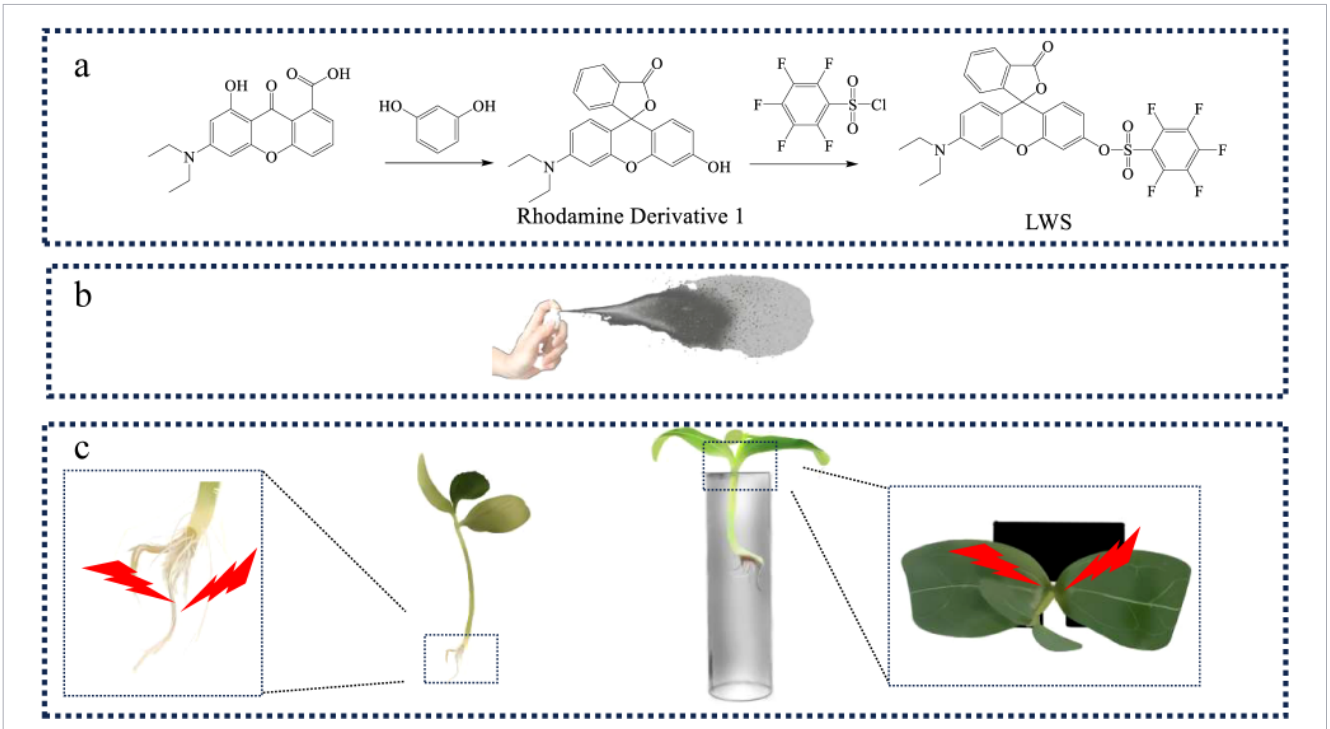

FIGURE 1
(a) Step 1: Synthesis of the fluorescent probe, **(b)** Step 2: Application of the fluorescent probe solution to plants using a small sprayer, **(c)** Step 3: Fluorescence imaging and photography.

Bruker Corporation), high-resolution mass spectrometer (Xevo G2-XS Qtof, Waters Corporation), mass spectrometer (LTQ Orbitrap Elite, Thermo Fisher Scientific), *In vivo* plant imaging system (IVIS Lumina LT, PerkinElmer, USA), UV-Vis spectrophotometer (TU-1901, Persee), and fluorescence spectrophotometer (RF-5301 PC, Shimadzu Corporation). All chemicals and solvents were commercially available and used without further purification.

2.2 Synthesis of the compound

2.2.1 Synthesis of rhodamine derivative 1

A mixture of 1.00 g of 2-[4-(diethylamino)-2-hydroxybenzoyl] benzoic acid and 0.35 g of resorcinol was added to a round-bottom flask and dissolved in 8 mL of trifluoroacetic acid (TFA). The reaction mixture was heated to 90 °C under stirring for 24 h. The solvent was subsequently removed under reduced pressure using a rotary evaporator, yielding a crude solid product. Purification via silica gel column chromatography with an ethyl acetate/petroleum ether eluent system (5:3, v/v) afforded a reddish-brown solid (1.13 g, yield: 90%).

^{1}H NMR (600 MHz, DMSO-d_6) δ 8.15 (d, J = 7.7 Hz, 1H), 7.85 (td, J = 7.5, 1.3 Hz, 1H), 7.78 (td, J = 7.6, 1.2 Hz, 1H), 7.41 (d, J = 7.5 Hz, 1H), 7.01 (s, 1H), 6.90 (dq, J = 28.3, 12.6, 9.2 Hz, 5H), 1.18 (t, J = 7.0 Hz, 6H).

^{13}C NMR (151 MHz, DMSO-d_6) δ 167.69, 159.21, 158.93, 158.66, 158.38, 155.05, 134.26, 131.10, 130.88, 130.77, 117.86, 115.93, 115.52, 102.60, 97.02, 45.58, 12.91.

MS: Calcd for $[C24H21NO4]^+$ 387.1500, found $[M + H]^+$ 388.3420.

2.2.2 Synthesis of the fluorescent probe LWS

Rhodamine derivative 1 (1.00 g) was accurately weighed and dissolved in a stoichiometric volume of dichloromethane (DCM) in a round-bottom flask, which was then immersed in an ice-water bath. Under continuous stirring, triethylamine (0.39 g) was added dropwise. After 10 min, a dichloromethane solution (20 mL) containing pentafluorobenzenesulfonyl chloride (0.84 g) was slowly added to the reaction mixture via an addition funnel over 30 min. Following complete addition, the ice bath was removed, and the mixture was stirred at ambient temperature (25°C) for 12 h. The reaction solvent was evaporated under reduced pressure using a rotary evaporator to obtain the crude product. Purification through column chromatography with a dichloromethane/petroleum ether gradient (5:1, v/v) yielded the target probe LWS as a pink crystalline solid (1.02 g, 64% yield).

^{1}H NMR (600 MHz, $CDCl_3$) δ 8.05 (d, *J* = 7.5 Hz, 1H), 7.71 (td, *J* = 7.5, 1.3 Hz, 1H), 7.23-7.18 (m, 2H), 6.87 (dd, *J* = 8.7, 2.4 Hz, 1H), 6.82 (d, *J* = 8.8 Hz, 1H), 6.60 (d, *J* = 8.9 Hz, 1H), 6.51 (s, 1H), 6.46 - 6.40 (m, 1H), 3.40 (q, *J* = 7.1 Hz, 4H), 1.21 (t, *J* = 7.0 Hz, 6H).

^{13}C NMR (151 MHz, $CDCl_3$) δ 169.28, 152.64, 152.51, 152.48, 152.15, 151.96, 149.46, 142.78, 139.29, 135.91, 135.18, 135.12, 131.17, 130.07, 129.91, 128.87, 126.92, 125.14, 124.78, 124.02, 123.49, 119.78, 116.12, 115.91, 114.08, 110.20, 29.71, 29.66, 14.13, 12.42.

MS: Calcd for $[C30H20F5NO6S]^+$ 617.0931, found $[M + H]^+$ 618.1035.

The ^{1}H NMR, ^{13}C NMR spectra and mass spectra of the compounds are shown in support information.

2.3 Spectrophotometric measurement and selectivity analysis

A stock solution of probe LWS (10 mmol/L) was prepared by dissolving the appropriate quantity of LWS in dimethyl sulfoxide (DMSO). A 30% H_2O_2 solution was diluted with distilled water to obtain a 10 mmol/L H_2O_2 stock solution, which was freshly prepared prior to each experiment. The 10 mmol/L H_2O_2 stock solution was serially diluted to concentrations ranging from 0 to 100 μmol/L. These diluted H_2O_2 solutions were then mixed with the LWS probe solution (20 μmol/L in PBS: DMSO (1:1, v/v)) for subsequent analyses.

The pH of the probe LWS solution was adjusted using standardized hydrochloric acid (HCl) or sodium hydroxide (NaOH) solutions, covering a pH range of 3.0 to 11.0.

Selectivity experiments for plant hormones, ions, and various ROS were conducted. Plant hormones were dissolved in DMSO, while ions and other ROS were dissolved in distilled water. Fluorescence of LWS before and after the addition of analytes was monitored under an excitation wavelength of 522 nm. For other ROS, singlet oxygen ($^1O_2$, 50 mmol/L) was generated by adding H_2O_2 (500 mmol/L) to a sodium molybdate (50 mmol/L) solution. $\cdot O_2^-$ was produced by reacting 300 μmol/L xanthine with 10 mU/mL xanthine oxidase. ·OH (50 mmol/L) were generated by adding H_2O_2 (500 mmol/L) to a ferrous sulfate (50 mmol/L) solution. Nitric oxide (50 mmol/L) was prepared by dissolving 149 mg of sodium nitroprusside (SNP) in deionized water to a final volume of 10 mL. Tert-butyl hydroperoxide (TBHP, 50 mmol/L) solution was prepared by diluting 69 μL of 70% tert-butyl hydroperoxide with deionized water to 10 mL. During spectral measurements, the excitation wavelength was set at 522 nm, and the fluorescence emission spectra were recorded from 540 to 800 nm.

2.4 Toxicity experiment of the fluorescent probe on plants

Bottle gourd seeds were soaked in water at 55°C for 10 minutes, then transferred to fresh water and soaked overnight at room temperature. The seeds were subsequently germinated in a 32°C incubator. Once radicles emerged, the seeds were sown into 32-cell seedling trays. When the seedlings reached the two-leaf and one-heart stage, bottle gourd seedlings of similar size were selected for toxicity tests. The experimental groups included a control group (deionized water, CK) and treatment groups (10-100 μmol/L probe

concentrations), with three replicates per group. After hydroponic culture for 72 hours, root length, stem length, stem diameter, fresh weight, and dry weight were measured.

2.5 Visualization imaging of H_2O_2 in plants

Seeds of Bottle gourd, Tomato(*Solanum Lycopersicum L.*), Pumpkin(*Cucurbita* spp.), and Melon(*Cucumis melo L.*) were raised into seedlings following the procedures described in Section 2.4. Littleleaf boxwood(*Buxus microphylla.*) and Orange (*Citrus reticulata.*) were obtained from the planting base.

After washing the root substrates from all plants, size and vigor-matched individuals were cultured in Hoagland nutrient solution until they acclimated to a hydroponic environment. Salt stress in Bottle gourd was imposed with 0, 50, or 100 mmol/L NaCl. Drought stress in Littleleaf boxwood was imposed with 0%, 10%, or 20% PEG6000. Cadmium stress in Orange was imposed with 0, 100, or 200 μmol/L $CdCl_2$. The stress duration for these three treatments was 24 h. Tomato was subjected to waterlogging using a solution containing 100.1 mg/L $KHCO_3$, 69.0 mg/L $MgSO_4$, and 91.7 mg/L $CaCl_2$, and H_2O_2 was measured at 0, 24, and 48 h after stress initiation. Each treatment had three replicates. At the preset stress time points, roots were rinsed three times with distilled water and then transferred to a solution containing the fluorescent probe for a 1 h incubation. Following incubation, the roots were rinsed three times with distilled water, and surface moisture was removed using absorbent paper. Fluorescence imaging was performed using the fluorescent mode of the IVIS Lumina LT *in vivo* imaging system. (excitation wavelength: 522 nm, emission wavelength: 552 nm). After imaging, to ensure the biological relevance of the fluorescence signal, an appropriate region of interest (ROI) was selected using Living Image software to calculate relative fluorescence intensity.

Bottle gourd cultivars H02 and H12, along with pumpkin NC03T, were used as rootstocks. When the seedlings reached the two-leaf and one-heart stage, grafting was performed using melon as the scion by the top-insertion method. H_2O_2 levels were monitored on days 1, 3, 5, and 7 after grafting, with three replicates per time point. A small sprayer was used to apply the fluorescent probe solution to the grafting site, and after 1 hour, imaging was performed using the IVIS Lumina LT *in vivo* imaging system. To ensure consistent imaging height, grafted seedlings were placed inside 12-cm-high glass tubes during imaging. Relative fluorescence intensity was quantified using the fluorescent mode of the IVIS Lumina LT by selecting a 0.3×0.4 cm ROI around the graft junction to calculate the total ROI values(excitation wavelength: 522 nm, emission wavelength: 552 nm), thereby ensuring the biological relevance of the fluorescence signal. In addition, hydrogen peroxide levels in grafted seedlings subjected to the same treatments were determined using a hydrogen peroxide assay kit (Solarbio, Cat: BC3590, Spectrophotometer, China) according to the manufacturer's instructions.

All data were obtained from three biological replicates (10 seedlings per replicate) and are expressed as relative fluorescence intensity (photons per second, p/s). Statistical analysis was performed using one-way analysis of variance (ANOVA) with Duncan's multiple range test for *post hoc* comparison of means, using SPSS software (version 27, IBM Corp.). Differences were considered statistically significant at $p < 0.05$. To eliminate differences in data scale between the two methods, the measurement data were normalized, and Bland–Altman analysis and Pearson's correlation coefficient were then used to evaluate the agreement between the method proposed in this study and the commercial kit-based assay.

3 Results

3.1 Synthesis of the fluorescent probe LWS

The synthetic route of probe LWS is illustrated in Figure 1a. The synthesis begins with a cyclization reaction under acidic conditions between the starting materials 2-(4-diethylamino)-2-hydroxybenzoylbenzoic acid and resorcinol, yielding the rhodamine derivative 1. Under basic conditions, compound 1 is subsequently reacted with pentafluorobenzenesulfonyl chloride to afford the target probe LWS as a pink solid (64% yield). The structures of rhodamine derivative 1 and LWS were confirmed by ^{1}H NMR, ^{13}C NMR, and HRMS spectroscopy (Supporting Information).

3.2 Response of probe LWS to H_2O_2 *in vitro*

The UV-visible absorption spectrum of the probe solution (Supplementary Figure 1) shows that probe LWS exhibits a characteristic absorption peak at 522 nm. As depicted in Figure 2a, the fluorescence spectrum of the probe solution was recorded using 522 nm-the wavelength of maximum absorption-as the excitation wavelength. Upon the addition of varying concentrations of H_2O_2, the fluorescence intensity at 552 nm increased significantly. To investigate the response speed of LWS toward H_2O_2, time-course fluorescence measurements were performed at various time points. As shown in Figure 2b, the fluorescence emission intensity stabilized after approximately 100 minutes upon the addition of H_2O_2. The pH within plant bodies generally ranges from 7.0 to 7.5, but depending on environmental conditions and different plant parts, the internal pH can vary from slightly acidic to slightly alkaline. To ensure that our fluorescent probe can react with H_2O_2 within plant bodies, we assessed the effect of different pH conditions on the probe's performance. As shown in Supplementary Figure 2, the fluorescent probe was able to react with H_2O_2 and emit fluorescence at 552 nm within the pH range of 6.0 to 8.0. To ensure that the probe's response aligns with the environmental and physiological pH conditions within plant bodies, we selected pH 7.4 for subsequent experiments (Felle, 1988; Yu et al., 2000) The response of probe LWS to varying concentrations of H_2O_2 is shown in Figure 2c. With increasing concentrations of H_2O_2, the fluorescence emission intensity increased accordingly. A good linear relationship was observed in the range of 0-100 μmol/L H_2O_2 ($R^2 = 0.9849$), with a regression equation of $y = 502.97267z \pm 35.00899[H_2O_2]$. The calculated limit

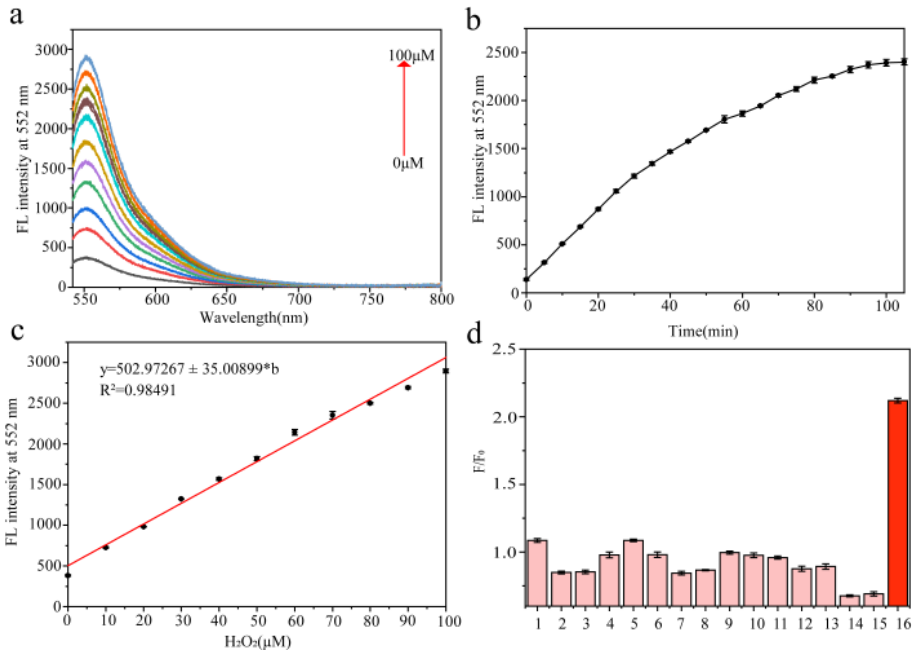

FIGURE 2
(a) Fluorescence spectrum of the LWS fluorescent probe with H_2O_2 (0-100 μmol/L), **(b)** Time dependence of the fluorescence probe on H_2O_2, **(c)** Linear relationship between fluorescence intensity at 552 nm and H_2O_2 concentration (0-100 μmol/L), **(d)** Fluorescence spectrum of the fluorescent probe in the presence of substances that may coexist with H_2O_2 in plants (1: $^1O_2$, 2: O_2^-, 3: ·OH, 4: NO·, 5: TBHP, 6: MeJA, 7: Abscisic acid, 8: Salicylic Acid, 9: Zeatin, 10: GA3, 11: IAA, 12: Ca^{2+}, 13: Fe^{2+}, 14: Fe^{3+}, 15: Catalase, 16: H_2O_2).

of detection (LOD) was 0.645 μmol/L. The specificity of probe LWS for H_2O_2 was further examined, as shown in Figure 2d. Among all tested species, LWS exhibited the most pronounced fluorescence response toward H_2O_2. In contrast, no significant fluorescence enhancement was observed upon the addition of other ROS ($^1O_2$, $\cdot O_2^-$, ·OH, NO·, TBHP); plant hormones that may coexist with H_2O_2 in plant bodies (methyl jasmonate, abscisic acid, salicylic acid, zeatin, auxin, gibberellin); representative cations (Ga^{2+}, Fe^{2+}, Fe^{3+}); or catalase.

To gain deeper insight into the response mechanism of the fluorescent probe LWS toward H_2O_2, comparative analysis was performed on the reaction residues of LWS with H_2O_2 using high-resolution mass spectrometry (HRMS). As shown in Figure 3a, in addition to the molecular ion peak of LWS (m/z 618.101), a new peak was observed at m/z 388.154, consistent with the formation of the reaction product LWS-1. This response mechanism was further investigated using density functional theory (DFT) calculations carried out with the Gaussian 16 software package, employing the B3LYP/6-31G(d,p) basis set. As shown in Figure 3b, for the unreacted LWS probe, the π-electron cloud of the LUMO orbital was mainly localized on the pentafluorobenzenesulfonyl group. Upon activation by H_2O_2 and conversion to LWS-1, this group was cleaved, and the electron cloud became delocalized over the entire fluorophore. Moreover, the LUMO-HOMO energy gap of the activated product LWS-1 (0.111 eV) was smaller than that of the unreacted probe LWS (0.129 eV).

3.3 Response of Probe LWS to H_2O_2 *in vivo*

3.3.1 Toxicity of the fluorescent probe on plants

Before investigating whether the fluorescent probe could be applied for *in vivo* imaging in plants, we conducted a phytotoxicity test on the fluorescent probe in living plants. As shown in Figure 4a, bottle gourd seedlings were treated with different concentrations of the fluorescent probe. Except for the seedlings treated with distilled water, whose roots retained their original color, those exposed to 10-100 μmol/L probe solutions had their roots in direct contact with the probe. During the three-day treatment, H_2O_2 produced by normal plant growth was continuously detected, and the reaction product of the fluorescent probe with H_2O_2 accumulated in the roots, resulting in the red coloration of the bottle gourd seedling root systems. To confirm that this color change does not affect the normal growth and development of plants, we measured the root length, stem length, stem diameter, fresh weight, and dry weight of bottle gourd seedlings (Figures 4b–f). Statistical analysis showed that at probe concentrations of 50 μmol/L or lower, neither the fluorescent probe nor its reaction product with H_2O_2 had a significant effect on the growth of either the aboveground or underground parts of the seedlings, nor did they significantly impact fresh or dry biomass. Therefore, to ensure maximal detection of H_2O_2 within plants without interfering with plant development, a probe concentration of 50 μmol/L was selected for subsequent applications in plant systems.

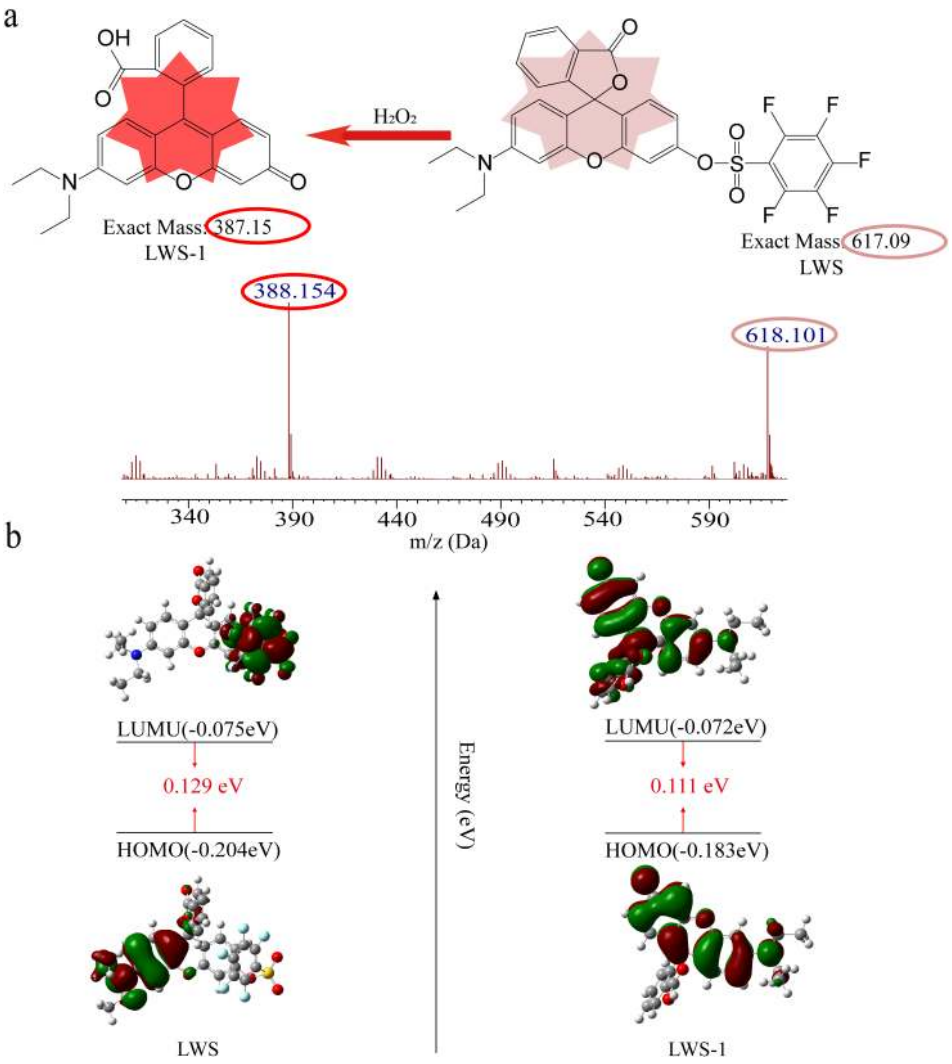

FIGURE 3
(a) Mass spectrum of the fluorescence probe LWS after reacting with the target H_2O_2, **(b)** DFT calculation of the frontier molecular orbital energy levels for LWS (left) and LWS-1 (right).

3.3.2 Detection of in plant H_2O_2 induced by experimentally controlled stress gradients using the fluorescent probe LWS

As shown in Figure 5a, in Bottle gourd, Tomato, Orange, and Littleleaf boxwood, low fluorescence was observed under no-stress conditions in the ck group, indicating that the fluorescent probe LWS detected endogenous H_2O_2 involved in maintaining normal growth and development. When these four species were subjected to different stress treatments, relative fluorescence intensity increased with increasing stress severity. As shown by statistical analysis of relative fluorescence intensity values in Figure 5b, for each species, pairwise comparisons among ck, group 1, and group 2 showed significant differences, and changes in relative fluorescence intensity were positively correlated with stress severity.

3.3.3 Detection of grafting-induced in plant H_2O_2 under non-controlled conditions using the fluorescent probe LWS

To validate the stem imaging performance of the fluorescent probe LWS and its ability to detect in plant H_2O_2 under non-controlled conditions, we combined it with grafting. As shown in Figure 6a, the grafted seedlings with the bottle gourd variety H02 as the rootstock exhibited a continuous increase in relative fluorescence intensity at the graft union as the grafting time progressed. For the grafted seedlings with the bottle gourd variety H12 as the rootstock, the relative fluorescence intensity on the third day was stronger than on the first day, while the relative fluorescence intensity on the fifth day was weaker than on the third day, and on the seventh day, the intensity increased again.

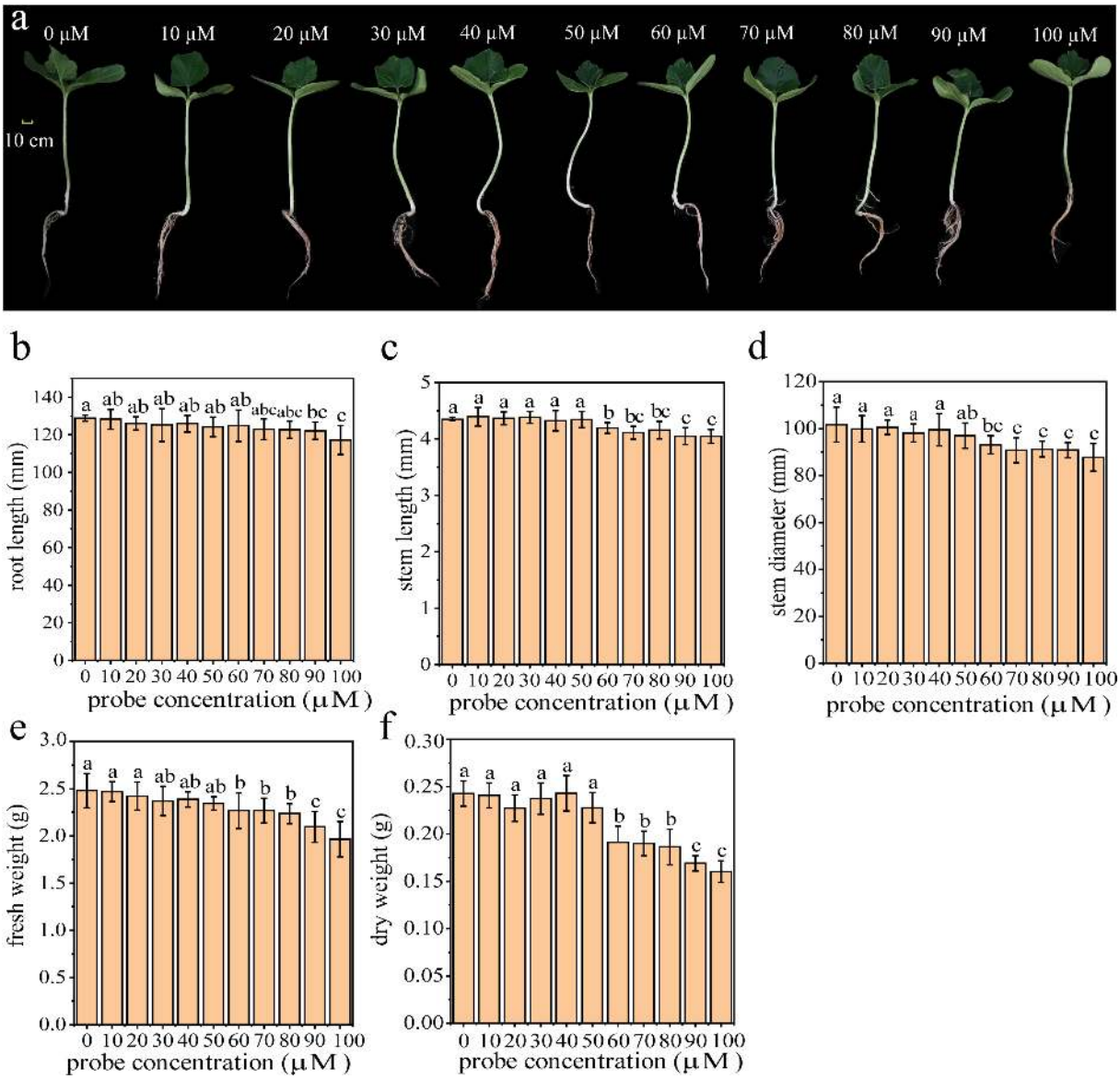

FIGURE 4
(a) Plant growth morphology, **(b)** Effect of 0-100 μmol/L fluorescent probe concentration on root length, **(c)** Effect of 0-100 μmol/L fluorescent probe concentration on stem length, **(d)** Effect of 0-100 μmol/L fluorescent probe concentration on stem diameter, **(e)** Effect of 0-100 μmol/L fluorescent probe concentration on fresh weight, **(f)** Effect of 0-100 μmol/L fluorescent probe concentration on dry weight.

Statistical analysis was performed on the relative fluorescence intensity produced at the graft union of samples with different rootstocks at different time points. (Figure 6b; Table 1). Between days 1 and 7, the relative fluorescence intensity of H_2O_2 in the grafted seedlings of the H02 variety exhibited more stable changes compared to those of the H12 variety. Subsequently, we calculated the grafting survival rates of the two cultivars, which were 94% for H02 and 64% for H12.

To verify that our fluorescent probe LWS can also be used in the stem of other plant, we used the pumpkin variety NC03T as the rootstock and the same melon (*Cucumis melo*) variety as the scion to monitor H_2O_2 dynamics over days 1-7. In the grafted seedlings with pumpkin as the rootstock, the average relative fluorescence intensity on day 1 was 1.68E + 08 p/s, which increased to a peak of 2.62E + 08 p/s on day 3, and then gradually decreased to 2.05E + 08 p/s. The mean values and standard deviations recorded from days 1 to 7 reflected variations in relative fluorescence intensity and fluctuations in signal levels over time. In addition, we employed a widely used commercial hydrogen peroxide assay kit to measure H_2O_2 levels in grafted seedlings subjected to the same treatments, and evaluated the agreement between our method and the commercial kit using Pearson's correlation coefficient and Bland-Altman analysis. (Millard et al., 2018; Munawar et al., 2019; Wecking et al., 2020) Pearson correlation analysis showed $r = 0.999$ ($p < 0.001$), with all data points lying close to the regression line (Supplementary Figure 3). Bland-Altman analysis further indicated a very small bias

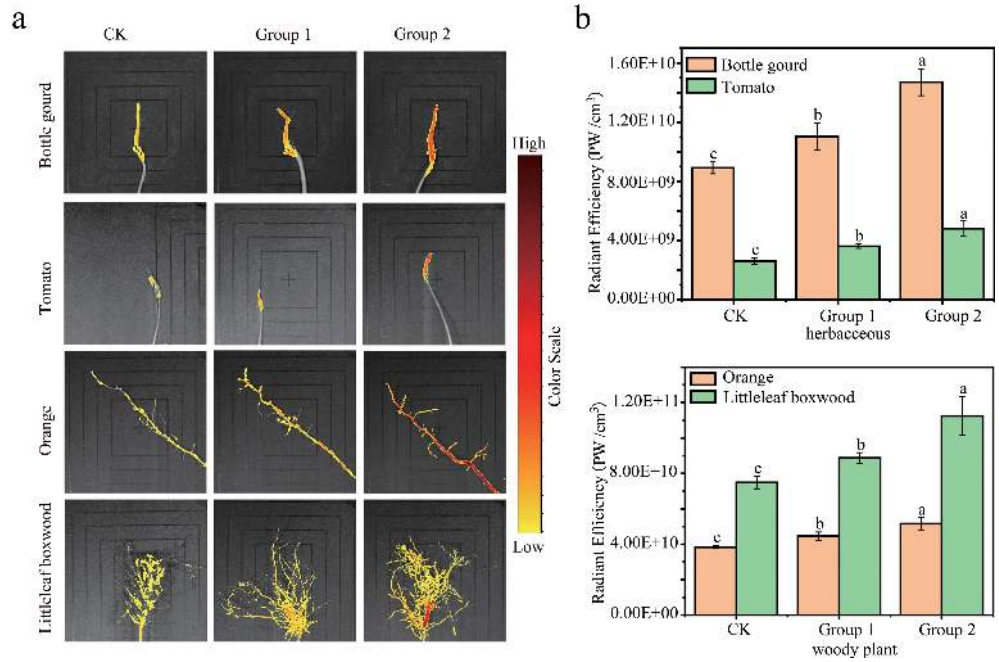

FIGURE 5
Fluorescence imaging of plant roots using the fluorescent probe LWS. **(a)** Bottle gourd under salt stress ck is the control, group 1 is 50 mmol/L NaCl, group 2 is 100 mmol/L NaCl, color scale from 1.00e8 μW/cm^2 to 1.00e9 μW/cm^2. Tomato under waterlogging stress ck is 0 h, group 1 is 12 h after treatment, group 2 is 24 h after treatment, color scale from 1.28e8 μW/cm^2 to 3.80e8 μW/cm^2. Orange under cadmium stress ck is the control, group 1 is 100 μmol/L $CdCl_2$, group 2 is 200 μmol/L $CdCl_2$, color scale from 1.45e8 μW/cm^2 to 1.35e9 μW/cm^2. Littleleaf boxwood under drought stress ck is the control, group 1 is 10% PEG6000, group 2 is 20% PEG6000, color scale from 1.70e8 μW/cm^2 to 2.18e9 μW/cm^2. **(b)** Relative fluorescence intensity was calculated for each species under different stress levels. For Bottle gourd, a 2*9 cm ROI was selected to compute fluorescence. For Tomato, a 2*4 cm ROI was selected to compute fluorescence. For Orange, a 10*10 cm ROI was selected to compute fluorescence. For Littleleaf boxwood, a 12*12 cm ROI was selected to compute fluorescence. Relative fluorescence intensity values are expressed as mean ± standard deviation, based on three independent replicates.

and narrow 95% limits of agreement, with all observations falling within these limits, demonstrating good agreement between our method and the commercial kit and supporting the practical applicability of the LWS fluorescent probe (Figure 6c).

4 Discussion

In this study, spectroscopy and theoretical analysis confirmed the activation mechanism behind the probe LWS. The probe LWS contains

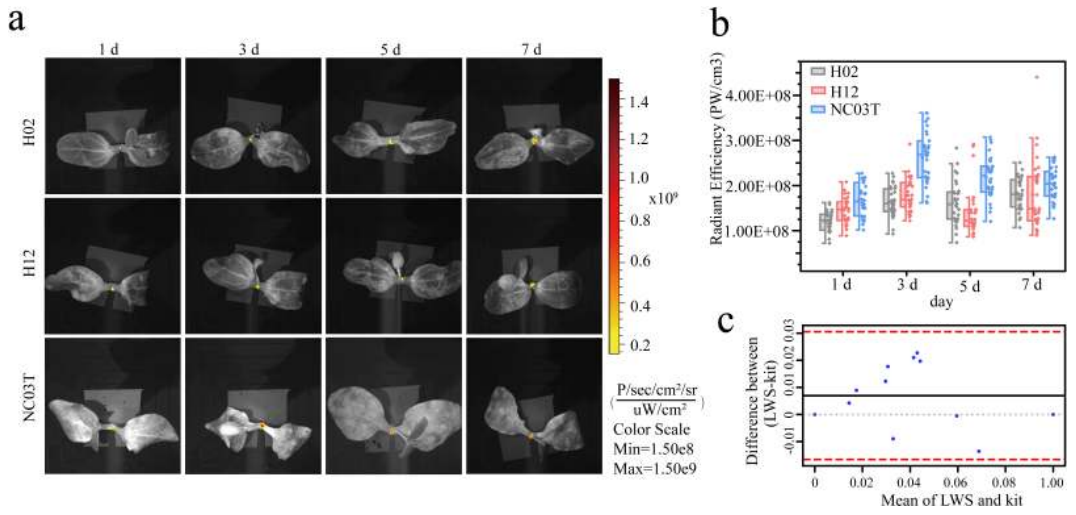

FIGURE 6
(a) Stem imaging of bottle gourd rootstocks H02, H12, and pumpkin rootstock NC03T at days 1, 3, 5, and 7 after grafting, color scale from 1.50E8 μW/cm^2 to 1.50E9 μW/cm^2. **(b)** Relative fluorescence intensity calculated from the selected 0.3*0.4 cm ROI area in the stem at different time points for different rootstocks, with a total of 30 samples per time point from three independent experiments. **(c)** Bland-Altman plot showing the agreement between the LWS fluorescent probe method and the commercial kit assay, with the red dashed lines representing the 95% limits of agreement and the black solid line representing the mean difference.

10.3389/fpls.2026.1767323

TABLE 1 Statistical table of relative fluorescence intensity at the graft union in different varieties.

Variety	Day	Mean value (p/s)	SD (p/s)	Median (p/s)
H02	1d	1.21E+08	2.18E+07	1.23E+08
H12	1d	1.45E+08	2.87E+07	1.47E+08
NC03T	1d	1.68E+08	3.68E+07	1.64E+08
H02	3d	1.63E+08	3.27E+07	1.60E+08
H12	3d	1.78E+08	3.76E+07	1.69E+08
NC03T	3d	2.62E+08	5.76E+07	2.69E+08
H02	5d	1.62E+08	4.81E+07	1.58E+08
H12	5d	1.41E+08	5.26E+07	1.22E+08
NC03T	5d	2.19E+08	4.67E+07	2.22E+08
H02	7d	1.82E+08	3.63E+07	1.81E+08
H12	7d	1.80E+08	7.83E+07	1.49E+08
NC03T	7d	2.05E+08	3.62E+07	2.04E+08

a rhodamine moiety with a conjugated electron system that enables efficient light absorption. However, the presence of a pentafluorobenzenesulfonyl group, which possesses strong electron-withdrawing properties, acts as a quenching group that reduces the fluorescence of the rhodamine core (Chen and Fang, 2023; Liu et al., 2023). Upon the addition of H_2O_2, H_2O_2 mediates the hydrolysis of the sulfonate, cleaving the pentafluorobenzenesulfonyl group from the rhodamine fluorophore. This cleavage eliminates the quenching effect of the pentafluorobenzenesulfonyl group, allowing the rhodamine fluorophore to revert to its native form. In this restored state, it exhibits a higher molar absorptivity in the ultraviolet region, resulting in an increase in UV absorption. Moreover, the removal of the quenching group restores the fluorophore to a more efficient fluorescent state, thereby enhancing both its absorption and emission properties. This enhancement is further supported by changes in electron cloud distribution and the LUMO-HOMO energy gap before and after the reaction of probe LWS with H_2O_2. Due to the strong electron-withdrawing effect of the pentafluorobenzenesulfonyl group in LWS, the π-electron cloud in the LUMO orbital is primarily localized on this group. Upon cleavage of the pentafluorobenzenesulfonyl group, the electron cloud becomes delocalized across the entire fluorophore scaffold. Additionally, the energy gap between the ground state and the excited state in the reaction product LWS-1 is smaller than that of the original probe LWS, allowing for more efficient excitation of electrons and resulting in enhanced fluorescence intensity.

Upon exposure to stress, plants activate a complex network of defense and adaptive responses, initiated by the rapid accumulation of reactive oxygen species as the primary signaling event. Through multi-layered regulatory mechanisms, this network subsequently coordinates key processes, including phytohormone signaling, cell wall remodeling, maintenance of redox homeostasis, and the activation of MAPK cascades, ultimately facilitating the perception, transduction, and response to environmental pressures. As a core signaling molecule, H_2O_2 not only triggers the reprogramming of stress-related gene expression by modulating redox states and activating MAPK cascades, but also forms a crucial "ROS-Ca^{2+} crosstalk" hub with second messengers like Ca^{2+} to regulate key enzyme activities. (Li et al., 2022b; Sood, 2025) This signaling module is intricately coupled with phytohormone networks, for instance, H_2O_2 and abscisic acid mutually amplify each other during stomatal regulation to promote closure and minimize water loss, while concurrently engaging in crosstalk with defense hormones such as jasmonic acid, salicylic acid, and ethylene. (Bharath et al., 2021) Furthermore, ROS accumulation activates both enzymatic and non-enzymatic antioxidant systems, which can partially mitigate the toxicity of the Fenton reaction by regulating interactions with transition metals like iron. (Dumanović et al., 2021) Subsequently, these biochemical and hormonal signals are manifested at the cellular structural level. In the apoplast, H_2O_2 is utilized by cell wall peroxidases to catalyze the oxidative cross-linking of phenolic compounds and hydroxyproline-rich glycoproteins, thereby enhancing cell wall rigidity and forming a physical barrier against pathogen invasion. (Mishler-Elmore et al., 2021; Ma, 2024) Collectively, these studies demonstrate that plant stress responses induce highly dynamic increases in the concentrations of a multitude of substances. These changes in non-H_2O_2 species increase the challenge of specifically recognizing H_2O_2 by fluorescent probes; therefore, in the design of probe LWS, a pentafluorobenzenesulfonyl group was introduced as the recognition unit. Due to its strong electronegativity, this group significantly enhances the probe's reactivity toward H_2O_2, enabling a highly selective response. This design enables the fluorescent probe to retain high specificity for H_2O_2 even within complex biological systems (Qi et al., 2025). In our results, probe LWS exhibited excellent selectivity for H_2O_2 and was not affected by abundant endogenous substances commonly coexisting with H_2O_2 in plants. These findings demonstrate that probe LWS retains its ability to recognize H_2O_2 in complex biological contexts, exhibiting excellent bioapplicability and high specificity.

Endogenous H_2O_2 accumulation in plants increases with the severity of stress, especially at early stages when H_2O_2 levels are positively correlated with stress intensity (Sachdev et al., 2021). In our results, across the four species tested under salt, drought, cadmium, and waterlogging stresses, fluorescence values rose significantly with increasing stress shortly after stress onset and exhibited a positive correlation with stress severity, consistent with the typical response pattern of plants under stress. This indicates that the fluorescent probe LWS can be used to detect the concentration of in plant H_2O_2 across different plants under various types of stress when stress intensity is experimentally controlled, demonstrating broad applicability.

Grafting is the process of joining two different plants to enhance crop disease resistance and quality, and it represents a form of plant tissue repair. During this process, plants with different graft compatibilities produce varying concentrations of H_2O_2 at the graft union site. Previous studies have indicated that cucurbit crops exhibit significant physiological and biochemical responses within the first 7 days following grafting, during which reactive oxygen species levels, including hydrogen peroxide, display marked differences. (Miao et al., 2021; Wang et al., 2025) Therefore, setting the measurement window for hydrogen peroxide content within 7 days after grafting is sufficient to effectively capture oxidative stress

responses during the early stage of grafting, and also allows verification of whether our method can detect hydrogen peroxide under complex and variable environmental conditions. It has been reported that oxidative bursts are commonly triggered during the initial phase of graft healing, whereas the antioxidant system is relatively compromised in incompatible grafts, thereby leading to greater H_2O_2 accumulation after wound healing than in compatible grafts (Aloni et al., 2008; Babar et al., 2023). Subsequently, callus formation likely began in the compatible grafts, and the associated increases in cell division, differentiation, and metabolic activity could have led to elevated H_2O_2 production (Irisarri et al., 2015; Carmach et al., 2023). In incompatible grafts, the antioxidant system is relatively weak and fails to scavenge H_2O_2 in a timely manner, meanwhile, delayed callus differentiation further contributes to the continued accumulation of H_2O_2 (Pina et al., 2012; Sofo et al., 2015; Babar et al., 2023). On day 5, the formation of active callus tissue and a robust antioxidant system in the compatible graft combination maintained a relative balance, resulting in no marked change in H_2O_2 accumulation. (Miao et al., 2019; He et al., 2025) In contrast, the callus tissue of the incompatible graft seedlings showed low cellular activity, allowing the antioxidant system to gradually remove the previously accumulated H_2O_2. (Thomas et al., 2024) By day 7 after grafting, vascular reconnection began to occur, which increased cellular activity at the graft union. As a result, the rate of H_2O_2 production exceeded its scavenging rate, leading to renewed H_2O_2 accumulation. (Feng et al., 2024) We observed that the fluorescence changes in Figure 6a were consistent with previous studies describing distinct stages during graft union healing. To further confirm that our method correctly captured the oxidative status at different stages in grafted seedlings, we analyzed the overall distribution of relative fluorescence intensity across the tested population and found that from day 1 to day 7 the mean relative fluorescence intensity of the compatible graft combination (H02) remained close to the median, indicating more concentrated and stable data. In contrast, for the incompatible graft (H12), although the mean on day 1 was close to the median, the means from days 3 to 7 deviated significantly from the median. Overall, the standard deviation of relative fluorescence intensity in the compatible rootstock H02 was smaller than that in the incompatible rootstock H12. Previous studies have suggested that, since H_2O_2 functions as a signaling molecule, the stability of its concentration may indicate how well plants coordinate wound responses and graft healing. In compatible grafts, a more efficient antioxidant system may rapidly establish homeostasis and maintain H_2O_2 at a controllable level for hormonal coordination during healing. (Rasool et al., 2020; Wang et al., 2024a) Conversely, physiological incompatibility between the rootstock and scion can cause inconsistent stress responses in incompatible grafts, resulting in heterogeneous physiological reactions during the healing process. (Babar et al., 2023; Wang et al., 2024a) These results indicate that the *in vivo* hydrogen peroxide patterns captured by our method are consistent with the trends and fluctuations observed in rootstocks with high versus low graft survival rates, and that our method remains effective for grafted seedlings under complex conditions where stress intensity is not artificially controlled. Whether in experimentally controlled settings or in grafting models that are more complex, challenging, and not artificially controlled, the fluorescent probe LWS exhibits great potential for screening individual plants with differing stress-response characteristics.

Notably, in Figure 6b, we observed that a subset of plants still exhibited H_2O_2-associated fluorescence intensities far above the population mean at the later stage, whereas another subset hovered below the mean level at the preceding time point. The pronounced individual-level variability within the same treatment group suggests that oxidative signals associated with graft union healing do not occur synchronously across plants. Moreover, the differences in relative fluorescence intensity among individuals within a population imply the importance of pre-screening individuals to reduce noise in biological studies. For physiological or omics studies that rely on conventional bulked sampling strategies, such "asynchronous individuals" are typically pooled indiscriminately into the same experimental group, which not only dilutes signals that are genuinely associated with healing efficiency or graft incompatibility, but may also obscure the expression patterns of key regulatory genes. By using the LWS probe–IVIS non-destructive detection platform established in this study, we are able to prospectively identify, without disturbing plant integrity, those individuals within the population that exhibit abnormally elevated or reduced H_2O_2 levels and to incorporate them into targeted follow-up experiments. More importantly, by imposing a mild stress on seedlings before field planting and then using our method to rapidly identify and select individuals with superior early-stage stress tolerance, pre-planting decisions can be greatly streamlined, resources wasted on poorly adapted plants can be minimized, and the overall uniformity of field stands as well as the consistency of crop performance can be improved.

Commercial H_2O_2 assay kits are widely used for the quantitative determination of hydrogen peroxide in plants. The hydrogen peroxide assay kit used in this study detects H_2O_2 based on the formation of a yellow peroxytitanium complex produced by the reaction between H_2O_2 and titanium sulfate, which shows a characteristic absorbance at 415 nm. The limit of detection (LOD) of the commercial kit is 0.002 μmol/L, which is lower than the 0.645 μmol/L of our method, enabling it to capture lower concentrations of hydrogen peroxide. However, both methods are capable of detecting the physiological values required to distinguish between stressed and unstressed plants. Regarding the linear range, the commercial kit operates between 0.0097 and 1.5 μmol/L. When this limited linear range is used to compare plants under severe oxidative stress conditions, reactive oxygen species accumulate significantly and H_2O_2 concentrations may exceed 1.5 μmol/L. This situation can easily lead to inaccurate comparisons of the oxidative status among highly stressed plants. Therefore, while the commercial kit is designed to detect trace amounts of hydrogen peroxide, the LWS probe retains sufficient sensitivity to detect biologically meaningful H_2O_2 elevations induced by stress, despite having a higher detection limit. Consequently, our method strikes an optimal balance between analytical sensitivity and the capacity to differentiate plants with varying oxidative states. While the commercial kit allows the quantitative determination of H_2O_2 concentration, its workflow

requires grinding plant tissues in an ice-water bath, which may cause H_2O_2 to degrade before reacting with the kit reagents. By contrast, our method preserves intact tissues, reducing the possibility of H_2O_2 degradation. Notably, the commercial kit destructively disrupts plant tissues, preventing the same samples from being used for subsequent studies. Although our method provides only semi-quantitative readouts of plant oxidative status, It lays the groundwork for subsequent investigations by enabling subsequent analyses on the same specimens. As shown in Supplementary Table 1, some previously reported sensors exhibit a wider linear range, while others achieve lower detection limits. (Bukhamsin et al., 2022; Park et al., 2023; Perdomo et al., 2023; Zhao et al., 2023; Li et al., 2024; Pan et al., 2024; Wang et al., 2024b; Zhang et al., 2025) However, the detection methods proposed in these studies generally involve some degree of physical injury to the plants; even when such damage is minimal, it may still disturb the individual plants and thereby affect the accuracy of subsequent experiments. Although our fluorescent probe is not the most outstanding in terms of analytical performance, it shows good applicability in plants, as demonstrated in Figures 5 and 6, which indicate that it is sufficient for screening individual plants. Importantly, the combination of this probe with our proposed detection method not only enables the identification of hydrogen peroxide, but also allows for the stratification of plants based on their oxidative status, thereby improving sample uniformity for downstream biological studies. Additionally, some non-destructive detection techniques based on spectroscopy or image recognition can significantly improve recognition accuracy when combined with machine learning algorithms, the phenotypic symptoms on which they rely often lag behind stress-induced physiological changes (Ji et al., 2025; Tuccio et al., 2025; Wu et al., 2025). Therefore, these approaches are more suitable for plant stress monitoring at the population scale or over large areas, rather than for precise early identification at the single-plant level. Consequently, in the early detection of plant stress, the timeliness of these sensors still remains clearly inferior to that of small-molecule fluorescent probes that undergo specific chemical reactions with defined physiological indicators. Spectroscopic evidence demonstrated that, in comparison with other small-molecule fluorescent probes, probe LWS provides H_2O_2 concentration readouts that approximately reflect the levels of H_2O_2 accumulated under stress conditions and enables highly specific detection of H_2O_2. In current literature, most fluorescent probe designs focus on rapid detection, typically completing target recognition within seconds or minutes. However, such designs may have limitations when applied to detecting endogenous H_2O_2 in plants under stress. When plants are subjected to stress, the accumulation of H_2O_2 within plant bodies varies among different cultivars. This differential accumulation modulates the responses of various plant hormones to stress, ultimately leading to distinct physiological outcomes in plant stress tolerance (Kamruzzaman et al., 2022) However, during the application of fluorescent probes in plants, factors such as environmental fluctuations, chemical treatments, and changes in endogenous enzyme activity or hormone levels may induce transient H_2O_2 peaks within plant bodies. Although plants possess efficient antioxidant systems that can rapidly eliminate such transient peaks, the H_2O_2 detected by rapid-response probes may include these suddenly occurring bursts and therefore cannot accurately reflect the true accumulation level of H_2O_2 induced by stress. Therefore, by controlling the reaction time, the LWS probe, while still enabling early detection, yields H_2O_2 levels that more closely approximate the accumulation concentration produced in plants under stress.

However, it should be noted that when the heights of the tested sites are not consistent, additional tools, such as the glass tubes used in this study, should be used to control the imaging height to ensure consistency in optical path length and excitation or emission efficiency, thereby eliminating noise caused by positional differences. In addition, because each imaging run of the IVIS *in vivo* imaging system requires a certain amount of time, it is not feasible to process a large batch of plants at once, otherwise differences in sample handling time will be introduced and result in technical noise. When measurements are performed using a standardized operating procedure, the standard deviation of the CK group in Figure 5b is smaller than that of the treatment groups, indicating that technical noise is effectively reduced and allowing the biological variation among individual plants to be observed. Because individual plants respond differently to stress, the treatment groups all show larger standard deviations. Figure 6b further demonstrates this, as incompatible grafted seedlings show a larger standard deviation. Due to the limited imaging chamber of the IVIS Lumina LT *in vivo* imaging system used in this study, this method is suitable for small plants but cannot accommodate large plants. Therefore, attention should be paid to the size of the target tissue to be measured. The physical limitation of tissue penetration depth remains a major challenge for small-molecule fluorescent probes. This limitation arises from the optical properties of biological tissues, such as light scattering and absorption, which cause the signal detected by IVIS *in vivo* imaging to mainly originate from superficial layers and thus fail to reflect H_2O_2 levels in deep tissues. (Hériché et al., 2022; Refaat et al., 2022) Accordingly, this method is limited to screening plants based on H_2O_2 levels generated in superficial tissues. A common challenge for the entry of exogenous substances into plants is that different abiotic stress types induce different degrees of stomatal closure and tissue permeability, thereby affecting probe penetration and in planta enrichment. (Li et al., 2022a; Yang et al., 2023) This reduces direct comparability across different stress types and restricts the method to comparing oxidative status only among plants subjected to the same type of stress, while limitations remain for comparisons between different stress types. In addition, consistent incubation time and washing steps are required to control probe enrichment in planta and to reduce interference from residual probe on the surface. Because our probe minimizes interference from transient fluctuations in H_2O_2 by controlling the reaction time, it measures the accumulated H_2O_2 level within the incubation window. Compared to other rapid detection methods, by integrating the signal over the incubation period, this method effectively filters out transient H_2O_2 fluctuations caused by minor environmental perturbations, chemical treatments, or changes in enzyme activity, thereby capturing the steady-state accumulation of

H_2O_2. Since the steady-state accumulation of H_2O_2 inherently serves as a crucial indicator of biological phenotypes, this approach provides more reliable data for evaluating long-term physiological stress, making it particularly suitable for studying chronic or prolonged stress states with enduring effects. It should be noted, however, that this also defines its application boundaries. When the research conditions or objectives require high-temporal-resolution and highly dynamic monitoring of stress responses, or necessitate pinpointing the exact temporal nodes of H_2O_2 signal transduction, this method fails to capture these instantaneous changes in hydrogen peroxide concentrations.

5 Conclusion

We have developed a novel fluorescent probe for H_2O_2 detection with excellent sensitivity and selectivity. This probe avoids transient H_2O_2 bursts caused by environmental stimuli or metabolic fluctuations in plants, thereby providing more reliable steady-state H_2O_2 measurements. Additionally, the probe functions effectively under physiological pH conditions found within plant tissues and exhibits no detrimental effects on plant growth and development at concentrations below 50 μmol/L. By applying the fluorescent probe LWS to different plants under various stress treatments, we observed that as stress severity increased, the relative fluorescence intensity detected by the IVIS Lumina LT *in vivo* imaging system rose with increasing oxidative stress, consistent with the typical response pattern of plants under stress. Similarly, when the fluorescent probe was applied to graft unions of seedlings from different cultivar combinations, statistical analyses showed relative fluorescence intensity changes consistent with earlier reports, and the measurements were consistent with the results obtained from a commercial kit. These results indicate that combining our H_2O_2 fluorescent probe with the IVIS Lumina LT imaging system and quantitative analysis using Living Image software enables precise quantification of relative fluorescence intensity across different plant tissues under various stresses. This method allows non-destructive screening of plants with similar physiological states, preserving plant integrity. Compared to traditional chemical detection methods, our approach maintains the integrity of plant tissues, facilitating subsequent omics and phenotypic analyses. In addition, before field cultivation, our method allows the selection of more stress-tolerant plant individuals, thereby ensuring crop yields under climate change conditions. In summary, our method provides a simple, effective, and non-destructive approach for measuring H_2O_2 concentrations in plants, laying a technical foundation for dissecting the regulatory networks underlying plant stress responses.

Data availability statement

The original contributions presented in the study are included in the article/Supplementary Material. Further inquiries can be directed to the corresponding author.

Author contributions

WL: Conceptualization, Data curation, Formal analysis, Methodology, Software, Validation, Writing – original draft, Writing – review & editing. HC: Formal analysis, Software, Writing – original draft. BZ: Formal analysis, Writing – original draft. QY: Formal analysis, Writing – original draft. XL: Formal analysis, Writing – original draft. JX: Formal analysis, Writing – original draft. TL: Formal analysis, Writing – original draft. JZ: Formal analysis, Writing – original draft. XC: Formal analysis, Writing – original draft. PW: Formal analysis, Writing – original draft. WY: Conceptualization, Funding acquisition, Project administration, Resources, Supervision, Writing – original draft, Writing – review & editing.

Funding

The author(s) declared that financial support was received for this work and/or its publication. This work was supported by the Guangxi Natural Science Foundation (2024JJA130134) and the Guangxi Natural Science Foundation (2024JJA130404).

Acknowledgments

We are grateful to Guangxi University.

Conflict of interest

The author(s) declared that this work was conducted in the absence of any commercial or financial relationships that could be construed as a potential conflict of interest.

Generative AI statement

The author(s) declared that generative AI was not used in the creation of this manuscript.

Any alternative text (alt text) provided alongside figures in this article has been generated by Frontiers with the support of artificial intelligence and reasonable efforts have been made to ensure accuracy, including review by the authors wherever possible. If you identify any issues, please contact us.

Publisher's note

All claims expressed in this article are solely those of the authors and do not necessarily represent those of their affiliated

organizations, or those of the publisher, the editors and the reviewers. Any product that may be evaluated in this article, or claim that may be made by its manufacturer, is not guaranteed or endorsed by the publisher.

Supplementary material

The Supplementary Material for this article can be found online at: https://www.frontiersin.org/articles/10.3389/fpls.2026.1767323/full#supplementary-material

References

Ahlawat, O. P., Yadav, D., Walia, N., Kashyap, P. L., Sharma, P., and Tiwari, R. (2024). Root exudates and their significance in abiotic stress amelioration in plants: a review. *J. Plant Growth Regul.* 43, 1736–1761. doi: 10.1007/s00344-024-11237-7

Aloni, B., Karni, L., Deventurero, G., Levin, Z., Cohen, R., Katzir, N., et al. (2008). Possible mechanisms for graft incompatibility between melon scions and pumpkin rootstocks. *Acta Hortic.* 782, 313–324. doi: 10.17660/ActaHortic.2008.782.39

Asaeda, T., Sanjaya, K., and Kaneko, Y. (2017). Effects of mechanical stressors caused by mean flow and turbulence on aquatic plants with different morphologies. *Ecohydrology* 10, e1873. doi: 10.1002/eco.1873

Babar, M., Afzal, N., Siddiqui, K., Azhar, A., and Galani, S. (2023). Exploring graft incompatibility markers: intraspecific and interspecific grafts of tomato (Solanum lycopersicum L.). *Sci. Hortic.* 310, 111762. doi: 10.1016/j.scienta.2022.111762

Bharath, P., Gahir, S., and Raghavendra, A. S. (2021). Abscisic acid-induced stomatal closure: an important component of plant defense against abiotic and biotic stress. *Front. Plant Sci.* 12. doi: 10.3389/fpls.2021.615114

Bukhamsin, A., Ait Lahcen, A., Filho, J. D. O., Shetty, S., Blilou, I., Kosel, J., et al. (2022). Minimally-invasive, real-time, non-destructive, species-independent phytohormone biosensor for precision farming. *Biosens. Bioelectron.* 214, 114515. doi: 10.1016/j.bios.2022.114515

Carmach, C., Castro, M., Peñaloza, P., Guzmán, L., Marchant, M. J., Valdebenito, S., et al. (2023). Positive effect of green photo-selective filter on graft union formation in tomatoes. *Plants* 12, 3402. doi: 10.3390/plants12193402

Chen, C., and Fang, C. (2023). Fluorescence modulation by amines: mechanistic insights into twisted intramolecular charge transfer (TICT) and beyond. *Chemosensors* 11, 87. doi: 10.3390/chemosensors11020087

Cortijo, S., Aydin, Z., Ahnert, S., and Locke, J. C. (2019). Widespread inter-individual gene expression variability in *Arabidopsis thaliana*. *Mol. Syst. Biol.* 15, e8591. doi: 10.15252/msb.20188591

Cotrina Cabello, G. G., Ruiz Rodriguez, A., Husnain Gondal, A., Areche, F. O., Flores, D. D. C., Astete, J. A. Q., et al. (2023). Plant adaptability to climate change and drought stress for crop growth and production. *CABI Rev.* 0004. doi: 10.1079/cabireviews.2023.0004

Dhoun, S., Kaur, S., Kaur, P., and Singh, K. (2017). A cyanostilbene-boronate based AIEE probe for hydrogen peroxide—application in chemical processing. *Sens. Actuators B* 245, 95–103. doi: 10.1016/j.snb.2017.01.143

Dumanović, J., Nepovimova, E., Natić, M., Kuča, K., and Jaćević, V. (2021). The significance of reactive oxygen species and antioxidant defense system in plants: a concise overview. *Front. Plant Sci.* 11. doi: 10.3389/fpls.2020.552969

Farooq, M. A., Niazi, A. K., Akhtar, J., Saifullah,, Farooq, M., Souri, Z., et al. (2019). Acquiring control: the evolution of ROS-induced oxidative stress and redox signaling pathways in plant stress responses. *Plant Physiol. Biochem.* 141, 353–369. doi: 10.1016/j.plaphy.2019.04.039

Felle, H. (1988). Short-term pH regulation in plants. *Physiol. Plant* 74, 583–591. doi: 10.1111/j.1399-3054.1988.tb02022.x

Feng, M., Augstein, F., Kareem, A., and Melnyk, C. W. (2024). Plant grafting: molecular mechanisms and applications. *Mol. Plant* 17, 75–91. doi: 10.1016/j.molp.2023.12.006

Hasanuzzaman, M., Parvin, K., Bardhan, K., Nahar, K., Anee, T. I., Masud, A. A. C., et al. (2021). Biostimulants for the regulation of reactive oxygen species metabolism in plants under abiotic stress. *Cells* 10, 2537. doi: 10.3390/cells10102537

He, Z., Zhang, Y., Xun, C., Zhang, Z., Ma, Y., Wei, X., et al. (2025). Analysis of the differences among Camellia oleifera grafting combinations in its healing process. *Plants* 14, 2432. doi: 10.3390/plants14152432

Henschel, J. M., Dias, T. J., De Moura, V. S., De Oliveira Silva, A. M., Lopes, A. S., Da Silva Gomes, D., et al. (2024). Hydrogen peroxide and salt stress in radish: effects on growth, physiology, and root quality. *Physiol. Mol. Biol. Plants* 30, 1175–1184. doi: 10.1007/s12298-024-01476-z

Hériché, M., Arnould, C., Wipf, D., and Courty, P.-E. (2022). Imaging plant tissues: advances and promising clearing practices. *Trends Plant Sci.* 27, 601–615. doi: 10.1016/j.tplants.2021.12.006

Irisarri, P., Binczycki, P., Errea, P., Martens, H. J., and Pina, A. (2015). Oxidative stress associated with rootstock–scion interactions in pear/quince combinations during early stages of graft development. *J. Plant Physiol.* 176, 25–35. doi: 10.1016/j.jplph.2014.10.015

Jennings, C., Baysal-Gurel, F., and Alexander, L. W. (2024). Powdery mildew of bigleaf hydrangea: biology, control, and breeding strategies for resistance. *Horticulturae* 10, 216. doi: 10.3390/horticulturae10030216

Ji, J., Lu, X., Ma, H., Jin, X., Jiang, S., Cui, H., et al. (2025). Estimation of plant leaf water content based on spectroscopy. *Front. Plant Sci.* 16. doi: 10.3389/fpls.2025.1609650

Kamruzzaman, M., Beyene, M. A., Siddiqui, M. N., Ballvora, A., Léon, J., and Naz, A. A. (2022). Pinpointing genomic loci for drought-induced proline and hydrogen peroxide accumulation in bread wheat under field conditions. *BMC Plant Biol.* 22, 584. doi: 10.1186/s12870-022-03943-9

Kirchner, P. H., Schramm, L., Ivanova, S., Shoyama, K., Würthner, F., and Beuerle, F. (2024). A water-stable boronate ester cage. *J. Am. Chem. Soc* 146, 5305–5315. doi: 10.1021/jacs.3c12002

Li, R., Liu, Z., Xiong, Y., Zhang, X., Chen, L., Li, D., et al. (2024). A smartphone-enabled colorimetric microneedle sensing platform for rapid detection of ascorbic acid in fruits. *ACS Appl. Mater. Interfaces* 16, 63941–63950. doi: 10.1021/acsami.4c15637

Li, S., Tan, T., Fan, Y., Raza, M. A., Wang, Z., Wang, B., et al. (2022a). Responses of leaf stomatal and mesophyll conductance to abiotic stress factors. *J. Integr. Agric.* 21, 2787–2804. doi: 10.1016/j.jia.2022.07.036

Li, Y., Liu, Y., Jin, L., and Peng, R. (2022b). Crosstalk between Ca2+ and other regulators assists plants in responding to abiotic stress. *Plants* 11, 1351. doi: 10.3390/plants11101351

Li, Y., Ren, L., Gao, T., Chen, T., Han, J., and Wang, Y. (2023a). A coumarin-based fluorescent probe for sensitive monitoring H2O2 in water and living cells. *Tetrahedron Lett.* 114, 154291. doi: 10.1016/j.tetlet.2022.154291

Li, Y., Sun, M., Wang, X., Zhang, Y.-J., Da, X.-W., Jia, L.-Y., et al. (2021). Effects of plant growth regulators on transient expression of foreign gene in Nicotiana benthamiana L. leaves. *Bioresour. Bioprocess.* 8, 124. doi: 10.1186/s40643-021-00480-5

Li, Y., Zhou, Y., Lei, J., Lu, Q., Qin, X., Xu, Q., et al. (2023b). A NIR fluorescent probe for the selective detection of hydrogen peroxide by acetyl-hydrolyzing in cells. *J. Mol. Struct.* 1271, 134042. doi: 10.1016/j.molstruc.2022.134042

Liang, T., Zhang, D., Hu, W., Tian, C., Zeng, L., Wu, T., et al. (2021). A dual lock-and-key two photon fluorescence probe in response to hydrogen peroxide and viscosity: application in cellular imaging and inflammation therapy. *Talanta* 235, 122719. doi: 10.1016/j.talanta.2021.122719

Liaqat, W., Altaf, M. T., Barutçular, C., Mohamed, H. I., Ali, Z., and Khan, M. O. (2024). Drought stress in sorghum: physiological tools, breeding technology, omics approaches and genomic-assisted breeding -a review. *J. Soil Sci. Plant Nutr.* 24, 1665–1691. doi: 10.1007/s42729-024-01702-3

Liu, Y., Chen, F., Sun, L., Zhang, Z., Chang, S., Zhang, J., et al. (2023). Influences of molecular structures on the spectral properties and photostability of rhodamine dyes. *Res. Chem. Intermed.* 49, 2417–2432. doi: 10.1007/s11164-023-05016-4

Ma, Q.-H. (2024). Lignin biosynthesis and its diversified roles in disease resistance. *Genes* 15, 295–305. doi: 10.3390/genes15030295

Miao, L., Li, S., Bai, L., Anwar, A., Li, Y., He, C., et al. (2019). Effect of grafting methods on physiological change of graft union formation in cucumber grafted onto bottle gourd rootstock. *Sci. Hortic.* 244, 249–256. doi: 10.1016/j.scienta.2018.09.061

Miao, L., Li, Q., Sun, T., Chai, S., Wang, C., Bai, L., et al. (2021). Sugars promote graft union development in the heterograft of cucumber onto pumpkin. *Hortic. Res.* 8, 146. doi: 10.1038/s41438-021-00580-5

Millard, D., Dang, Q., Shi, H., Zhang, X., Strock, C., Kraushaar, U., et al. (2018). Cross-site reliability of human induced pluripotent stem cell-derived cardiomyocyte based safety assays using microelectrode arrays: results from a blinded CiPA pilot study. *Toxicol. Sci.* 164, 550–562. doi: 10.1093/toxsci/kfy110

Mishler-Elmore, J. W., Zhou, Y., Sukul, A., Oblak, M., Tan, L., Faik, A., et al. (2021). Extensins: self-assembly, crosslinking, and the role of peroxidases. *Front. Plant Sci.* 12. doi: 10.3389/fpls.2021.664738

Mizuta, Y. (2021). Advances in two-photon imaging in plants. *Plant Cell Physiol.* 62, 1224–1230. doi: 10.1093/pcp/pcab062

Munawar, H., Safaryan, A. H. M., De Girolamo, A., Garcia-Cruz, A., Marote, P., Karim, K., et al. (2019). Determination of fumonisin B1 in maize using molecularly imprinted polymer nanoparticles-based assay. *Food Chem.* 298, 125044. doi: 10.1016/j.foodchem.2019.125044

Muthamilarasan, M., Singh, N. K., and Prasad, M. (2019). "Multi-omics approaches for strategic improvement of stress tolerance in underutilized crop species: a climate change perspective," in *Advances in Genetics* (Amsterdam, Netherlands: Elsevier), 1–38. doi: 10.1016/bs.adgen.2019.01.001

Mutka, A. M., and Bart, R. S. (2015). Image-based phenotyping of plant disease symptoms. *Front. Plant Sci.* 5. doi: 10.3389/fpls.2014.00734

Nazir, F., Fariduddin, Q., and Khan, T. A. (2020). Hydrogen peroxide as a signalling molecule in plants and its crosstalk with other plant growth regulators under heavy metal stress. *Chemosphere* 252, 126486. doi: 10.1016/j.chemosphere.2020.126486

Pan, Y., Tang, L., Li, L., Wu, X., and Yan, L. (2024). A versatile fluorescent probe for the ratiometric detection of hydrazine (N2H4) in water, soil, plant, and food samples. *Environ. pollut.* 359, 124766. doi: 10.1016/j.envpol.2024.124766

Park, J., Noh, H., Suh, H.-J., Ryu, D., Lee, H. J., and Lee, C. (2023). High-performance liquid chromatography using diode array detector and fluorescence detector for hydrogen peroxide analysis in processed fishery foods. *Food Sci. Biotechnol.* 32, 27–37. doi: 10.1007/s10068-022-01165-1

Peng, Z., Cui, M., Chu, J., Chen, J., and Wang, P. (2024). A novel AIE fluorescent probe for the detection and imaging of hydrogen peroxide in living tumor cells and in *vivo*. *Bioorg. Chem.* 150, 107592. doi: 10.1016/j.bioorg.2024.107592

Perdomo, S. A., de la Paz, E., Del Caño, R., Seker, S., Saha, T., Wang, J., et al. (2023). Non-invasive *in-vivo* glucose-based stress monitoring in plants. *Biosens. Bioelectron.* 231, 115300. doi: 10.1016/j.bios.2023.115300

Pina, A., Errea, P., and Martens, H. J. (2012). Graft union formation and cell-to-cell communication via plasmodesmata in compatible and incompatible stem unions of Prunus spp. *Scientia Hortic.* 143, 144–150. doi: 10.1016/j.scienta.2012.06.017

Qi, P., Zhang, Q., Ma, Y., Zhang, X., Ren, H., Hou, P., et al. (2025). Near-infrared fluorescent probe for real time detection of hydrogen peroxide in diabetic hepatopathy with enhanced sensitivity and specificity. *Microchem. J.* 215, 114458. doi: 10.1016/j.microc.2025.114458

Rasool, A., Mansoor, S., Bhat, K. M., Hassan, G. I., Baba, T. R., AlYemeni, M. N., et al. (2020). Mechanisms underlying graft union formation and rootstock scion interaction in horticultural plants. *Front. Plant Sci.* 11. doi: 10.3389/fpls.2020.590847

Refaat, A., Yap, M. L., Pietersz, G., Walsh, A. P. G., Zeller, J., Del Rosal, B., et al. (2022). *In vivo* fluorescence imaging: success in preclinical imaging paves the way for clinical applications. *J. Nanobiotechnol.* 20, 450–472. doi: 10.1186/s12951-022-01648-7

Sachdev, S., Ansari, S. A., Ansari, M. I., Fujita, M., and Hasanuzzaman, M. (2021). Abiotic stress and reactive oxygen species: generation, signaling, and defense mechanisms. *Antioxidants* 10, 277. doi: 10.3390/antiox10020277

Saxena, I., Srikanth, S., and Chen, Z. (2016). Cross talk between H2O2 and interacting signal molecules under plant stress response. *Front. Plant Sci.* 7. doi: 10.3389/fpls.2016.00570

Schupp, E. W., Zwolak, R., Jones, L. R., Snell, R. S., Beckman, N. G., Aslan, C., et al. (2019). Intrinsic and extrinsic drivers of intraspecific variation in seed dispersal are diverse and pervasive. *AoB Plants* 11, plz067. doi: 10.1093/aobpla/plz067

Sharova, E. I., Smolikova, G. N., and Medvedev, S. S. (2023). Determining hydrogen peroxide content in plant tissue extracts. *Russ. J. Plant Physiol.* 70, 216. doi: 10.1134/S1021443724603744

Shulaev, V., Cortes, D., Miller, G., and Mittler, R. (2008). Metabolomics for plant stress response. *Physiol. Plant* 132, 199–208. doi: 10.1111/j.1399-3054.2007.01025.x

Slesak, I., Libik, M., Karpinska, B., Karpinski, S., and Miszalski, Z. (2007). The role of hydrogen peroxide in regulation of plant metabolism and cellular signalling in response to environmental stresses. *Acta Biochim. Pol.* 54, 39–50. doi: 10.18388/abp.2007_3267

Sofo, A., Scopa, A., Nuzzaci, M., and Vitti, A. (2015). Ascorbate peroxidase and catalase activities and their genetic regulation in plants subjected to drought and salinity stresses. *Int. J. Mol. Sci.* 16, 13561–13578. doi: 10.3390/ijms160613561

Sood, M. (2025). Reactive oxygen species (ROS): plant perspectives on oxidative signalling and biotic stress response. *Discov. Plants* 2, 187. doi: 10.1007/s44372-025-00275-4

Thomas, H. R., Gevorgyan, A., Hermanson, A., Yanders, S., Erndwein, L., Norman-Ariztía, M., et al. (2024). Graft incompatibility between pepper and tomato elicits an immune response and triggers localized cell death. *Hortic. Res.* 11, uhae255. doi: 10.1093/hr/uhae255

Tibebu, B., and Nuh, B. (2019). Biotechnological tools for detection, identification and management of plant diseases. *Afr. J. Biotechnol.* 18, 797–807. doi: 10.5897/AJB2018.16591

Tuccio, L., Cacini, S., Arati, G., Distefano, C., Traversari, S., Fontanelli, G., et al. (2025). Integrating raman spectroscopy and optical meters for nitrogen management in broccoli seedlings. *Front. Plant Sci.* 16. doi: 10.3389/fpls.2025.1613503

Wang, L., Liao, Y., Liu, J., Zhao, T., Jia, L., and Chen, Z. (2024a). Advances in understanding the graft healing mechanism: a review of factors and regulatory pathways. *Hortic. Res.* 11, uhae175. doi: 10.1093/hr/uhae175

Wang, Y., Liu, Y., Liu, B., Yuan, Y., Wei, L., Wang, M., et al. (2023). A benzil- and BODIPY-based turn-on fluorescent probe for detection of hydrogen peroxide. *Molecules* 29, 229. doi: 10.3390/molecules29010229

Wang, X.-Y., Wang, Y.-J., Lin, Y.-M., Sun, X.-Y., Wu, Y.-Q., and Fu, Y.-L. (2024b). Based on BODIPY fluorescent probe for detecting NO in tumour cells, Zebrafish and rice roots under abiotic stresses. *Sens. Actuators B* 418, 136244. doi: 10.1016/j.snb.2024.136244

Wang, X., Xiong, M., Xu, J., Zhang, T., Kadeer, A., Bie, Z., et al. (2025). PIN1a-mediated auxin release from rootstock cotyledon contributes to healing in watermelon as revealed by seeds soaking-VIGS and cotyledon grafting. *Hortic. Res.* 12, uhae329. doi: 10.1093/hr/uhae329

Watahiki, M., and Trewavas, A. (2019). Systems, variation, individuality and plant hormones. *Prog. Biophys. Mol. Biol.* 146, 3–22. doi: 10.1016/j.pbiomolbio.2018.10.001

Wecking, A. R., Cave, V. M., Liáng, L. L., Wall, A. M., Luo, J., Campbell, D. I., et al. (2020). A novel injection technique: using a field-based quantum cascade laser for the analysis of gas samples derived from static chambers. *Atmos. Meas. Tech.* 13, 5763–5777. doi: 10.5194/amt-13-5763-2020

Wu, Y., Li, Z., and Shen, Y. (2019). A novel ESIPT phthalimide-based fluorescent probe for quantitative detection of H_2O_2. *ACS Omega* 4, 16242–16246. doi: 10.1021/acsomega.9b02594

Wu, X., Zhong, L., Ding, R., Wang, C., Chen, H., Zhong, S., et al. (2025). Non-destructive estimation of SPAD and biomass in Lamiophlomis rotata using hyperspectral imaging and deep learning with DRSA-CARS feature selection. *Front. Plant Sci.* 16. doi: 10.3389/fpls.2025.1640779

Yang, X., Zhang, Q., Zhang, S., Lai, M., Ji, X., Ye, Y., et al. (2023). Molecule fluorescent probes for sensing and imaging analytes in plants: developments and challenges. *Coord. Chem. Rev.* 487, 215154. doi: 10.1016/j.ccr.2023.215154

Yin, Y., Wang, G., Liu, Y., Wang, X.-F., Gao, W., Zhang, S., et al. (2022). Simple phenotypic sensor for visibly tracking H2O2 fluctuation to detect plant health status. *J. Agric. Food Chem.* 70, 10058–10064. doi: 10.1021/acs.jafc.2c02170

Yu, Q., Tang, C., and Kuo, J. (2000). A critical review on methods to measure apoplastic pH in plants. *Plant Soil* 219, 29–40. doi: 10.1023/A:1004724610550

Zhang, Y., Wei, H., Li, Y., Shang, Z., Zhang, R., Zhang, Z., et al. (2025). An azacrown ether-based near-infrared fluorescent probe for the detection of Pb2+ and its applications in food, environmental water, plant and animal samples. *Anal. Chim. Acta* 1351, 343882. doi: 10.1016/j.aca.2025.343882

Zhao, K., Xie, R., Zhou, Z., Chen, S., Zhu, X., Wu, C., et al. (2023). A turn-on NIR fluorescent probe for risk-assessing oxidative stress in cabbage roots under abiotic stress. *Talanta* 258, 124402. doi: 10.1016/j.talanta.2023.124402